Development of Metal-Supported Solid Oxide Fuel Cells with Exceptionally High Power Density for Range Extender Systems

David Udomsilp[1,2,*], Jürgen Rechberger[1,3], Raphael Neubauer[1,3], Cornelia Bischof[1,2,4], Florian Thaler[1,2], Wolfgang Schafbauer[1,4], Norbert H. Menzler[2], L.G.J. de Haart[2], Andreas Nenning[1,5], Alexander K. Opitz[1,5,*], Olivier Guillon[2,6], Martin Bram[1,2,7,*]

[1] Christian Doppler Laboratory for Interfaces in Metal-Supported Electrochemical Energy Converters, 52425 Jülich, Germany and 1060 Vienna, Austria

[2] Forschungszentrum Jülich GmbH, Institute of Energy and Climate Research, 52425 Jülich, Germany

[3] AVL List GmbH, Hans-List-Platz 1, 8020 Graz, Austria

[4] Plansee SE, 6600 Reutte, Austria

[5] TU Wien, Institute of Chemical Technologies and Analytics, Getreidemarkt 9/164-EC, 1060 Vienna, Austria

[6] Jülich Aachen Research Alliance: JARA-ENERGY, 52425 Jülich, Germany

[7] Lead contact

* Correspondence:
m.bram@fz-juelich.de, d.udomsilp@fz-juelich.de, alexander.opitz@tuwien.ac.at

SUMMARY

Solid oxide fuel cells (SOFCs) exhibit potential to become a key technology for future clean energy systems. The metal-supported SOFC deploys decisive strengths like fast start-up capability, mechanical robustness, and acceptable cost, making it the concept of choice for mobile applications. As most promising example, SOFC-powered range extenders for electric vehicles offer fast refuelling and significantly increased driving range, while lowering size, weight, and cost of the vehicle's battery. Here we report on the development of a metal-supported SOFC aiming at exceptionally high power density. A knowledge-based improvement of all electrochemically active cell components enables a performance increase up to a factor of 10 and demonstrates the effectiveness of target-oriented optimization of processing and microstructure. Ultimately, enhanced cells meet the industrial performance target by providing a current density of 2.8 A·cm^{-2} at 650 °C and 0.7 V and set a new benchmark for SOFC performance.

INTRODUCTION

Clean electricity generation based on renewables is of vital importance for realizing the international goals set with regard to CO_2 emissions and air pollution in order to limit the global temperature increase caused by greenhouse gases. As reported recently by the International Energy Agency IEA (https://www.iea.org), the mobility sector is a substantial contributor to these emissions, with 24 % of the energy-related CO_2 emissions worldwide in 2016. Therefore, significant impact can be achieved by developing alternative powertrains [1]. Whereas the high efficiency of batteries promotes their application, charging time, size, weight, and cost of batteries remain issues still limiting their widespread application [2,3]. Furthermore, large-scale electrification of the individual transport sector based on battery vehicles may be a substantial challenge for power grids, since they need to be capable of satisfying the immense demand of electricity, especially in large urban areas [3].

A promising concept to overcome these restrictions is the application of a range extender system continuously recharging a small-sized battery [2,4,5]. The fuel cell technology in general and solid oxide fuel cells (SOFCs) in particular are exceptionally well-suited to power automotive range extenders due to their superior efficiency compared to combustion engines, silent operation, and fast refuelling. Moreover, systems powered by SOFCs, which work at temperatures of 500-800°C, feature remarkable fuel flexibility. This flexibility allows for operation on almost every kind of reformed fuels, as high CO levels can be tolerated [6,7]. Thereby, the SOFC technology breaks free

from the restrictions of lacking hydrogen infrastructure, making it both an excellent candidate for the intermediate stage of using existing infrastructure as well as for the operation on biofuels or synthetic CH_4 and also green hydrogen produced from renewables in the future [2,4,8-10]. Consequently, SOFC-based range extenders combine the attractiveness of battery electric vehicles with the convenience of liquid fuels. The high efficiency of electrochemical energy conversion directly corresponds to lower CO_2 emission and enables a virtually particulate-free exhaust gas.

For a near-future realization of range-extender-based electric vehicles, quite stringent boundary conditions such as quick start-up, large fuel flexibility, long service life, high efficiency, and high power output have to be met to economically compete with currently available power train systems. AVL List GmbH defined the following target performance values that have to be met for SOFC-based range extender systems to on the one hand be economically competitive with existing systems and on the other hand to be technologically realizable yielding a market-ready system within the next years [2,4,5]:

- Operation at T < 700°C on i.) liquid hydrocarbon fuels for quick refuelling based on existing fuel distribution infrastructure and ii.) green H_2 in the future.
- Quick start-up of the range extender in less than 15 min.
- Lifetime > 10,000 h of operation, resulting in service intervals accepted by customers.
- System efficiency > 50 %.
- Power output ≥ 15 kW as a prerequisite for long-distance over-land driving.
- Current density – single-cell > 2.0 $A \cdot cm^{-2}$
- Current density – stack > 0.8 $A \cdot cm^{-2}$
- Volumetric power density – stack 1,000 – 1,200 $W \cdot L^{-1}$
- Volumetric power density – system 100 – 120 $W \cdot L^{-1}$
- Gravimetric power density – system 120 – 140 $W \cdot kg^{-1}$
- Degradation rate < 6 $mV \cdot kh^{-1}$
- Cost stack < 100 $€ \cdot kW^{-1}$
- Cost system < 200 $€ \cdot kW^{-1}$

These boundary conditions are in accordance with the targets of the US Department of Energy (DOE) Fuel Cells Technologies Office Multi-Year Research, Development, and Demonstration Plan (FCTO-MYRD&D) [11]. This plan defines technical targets for SOFC based auxiliary power units (APUs). DOE targets are dealing more with application of SOFC APUs in heavy trucks,

trains, aircraft or ships and were e.g. used by company Delphi to evaluate their progress of doing pioneering work in the field of APUs for heavy truck applications [12]. Nevertheless, application of APUs as range extender for battery electric vehicles was already mentioned in the early works of Botti et al. [12,13]. Since in heavy-duty and transportation sector the available space is less restricted than in battery electric vehicles, targets of AVL List GmbH are even more ambitious than DOE targets with respect to power density, system efficiency and costs.

From the currently known fuel cell types, the metal-supported SOFC has the highest potential to fulfil all these conditions [9]. High thermal conductivity and mechanical stability of ductile porous metal supports are the key to resist quick start-up cycles. Moreover, metal supports provide high robustness against vibrations and redox cycles, enable reduction of material costs, and ease joining, e.g. by welding [9,14,15]. However, this type of fuel cell is the newest addition to the family of solid oxide cells and thus still suffers from a couple of "teething problems" that need to be solved before metal-supported SOFCs are ready for an application in the mobile sector. In particular, volumetric as well as gravimetric power density, along with prolonged lifetime, remain the major challenges on the way to commercialization of metal-supported SOFCs in the automotive industry [2,4,16].

To overcome these challenges within a reasonable time frame, a target-oriented development of metal-supported SOFCs is required. Here, we report on a research concept, which is based on a strong synergy of theoretical electrochemical simulations, basic electrochemical studies of individual cell components, and advanced expertise in materials science and processing. Results from fundamental electrochemical studies were introduced in three steps in the cell concept of Plansee SE [17]. Some details of each optimization step have been already published before [18-21]. By combining all measures for the first time in one cell (here called generation three, Gen 3), we demonstrate an impressive power density of up to 3.13 $W \cdot cm^{-2}$ at 800 °C and 0.7 V, approaching an enhancement by a factor 10 compared to the reference [17,19]. Importantly, with a current density of 2.8 $A \cdot cm^{-2}$ at 650 °C, Gen 3 cells also meet the performance target of our industrial partner stated above. Preliminary tests hint on long-term stability of single-cells, which are operated under laboratory conditions for up to 1000 h. All cells used in this study are manufactured on industrial pilot scale with a cell size around 140 x 100 mm^2 from which smaller cells are laser-cut for basic electrochemical investigations. Our results reveal that metal-supported SOFCs with exceptionally high performance can truly be realized, making them utilizable for application in range extender systems, as e.g. developed by AVL List GmbH [2,4]. This breakthrough is achieved via a knowledge-based optimization of cell components enabled by the close collaboration of basic science and

advanced engineering. The importance of our results is emphasized by benchmarking with other cell concepts. In this context, it is important to highlight that this remarkable increase in power density is achieved by systematic improvement of microstructure and processing, without the need to introduce novel SOFC materials. Such progress is rarely reported in SOFC literature but of extremely high interest for decision-makers, manufacturers and end-users of SOFC technology, since it shows the potential of the used materials and the technology in general. Finally, the discussion of our results reveals that SOFC-based range extenders have great potential for being a key technology for electrification of our present transport and mobility sector. Furthermore, each optimization step has the potential to be implemented in other SOFC concepts, which may thus lead to improved performance of other SOFC applications as described in more detail in the Discussion as well.

RESULTS

Fundamental approach to boost electrochemical performance of Ni/GDC anodes

A knowledge-based improvement of the cell components in general and of the fuel electrode (i.e. the SOFC-anode) in particular was performed to exploit the full potential of metal-supported SOFCs. Since the metal substrate requires reducing sintering conditions, the processing of the fuel electrode is considerably different from established SOFC concepts and therefore needs individual development. This development was guided by a basic understanding of the employed materials and their interaction in the fuel electrode. Supported by experiments on model systems [22] as well as by electrochemical simulations [23], the polarization resistance of the anode was broken down to the level of physical elementary parameters. Linking experimental data, results of simulations, and materialographical investigations of the electrode, allowed identifying the most efficient approaches for minimization of the anode polarization resistance and thus was the key for maximizing the cell performance.

Unlike the pure ion conductor Yttrium doped zirconia (YSZ) in common SOFC anodes, Gadolinium doped ceria (GDC) is a mixed ionic electronic conductor (MIEC) under the reducing conditions at the fuel electrode [24,25]. Owing to its mixed valence of Ce^{3+}/Ce^{4+} it also acts as an excellent catalyst for the anodic fuel oxidation reaction, which proceeds on the entire GDC surface [26]. From this in-depth understanding of GDC's elementary properties and their role for the electrochemical reaction in the Ni/GDC cermet, we can deduce that the Ni phase is mainly necessary for the long-range electron transport and mechanical stability, whereas fine GDC

particles distributed over the Ni scaffold promote electro-catalytic activity as well as ion transport and local electron collection. This job-sharing situation is sketched in **Figure 1a** and can be modelled by a transmission-line-type equivalent circuit [23,27-30] that also considers the chemical capacitance of the GDC phase [31,32]. For fitting of impedance data (see below), elements considering (minor) resistive and capacitive effects of the electrode/electrolyte interface and the ohmic resistance of the electrolyte must be added; the resulting circuit is depicted in **Figure 1b**. From this circuit and the position of the resistors of the electrochemical reaction on the GDC surface and ion conduction in its bulk, it can be deduced that a high surface area and a low tortuosity of the GDC phase are crucial for a low anode polarization resistance.

Therefore, the optimized microstructure of our Ni/GDC anode is rather unconventional (see **Figure 2**) – the Ni phase is much coarser than the GDC phase and the anode thickness needs to be relatively large. This anode thus breaks two yet believed essential rules of SOFC anode processing: finely dispersed microstructure of both phases and limited thickness to avoid gas transport limitations. However, even if – in comparison to established SOFC anodes – sub-optimal at first glance, such structure perfectly exploits the potential of the used materials and the electrochemical reaction pathways in the cermet. As a consequence, the polarisation resistance of our Ni/GDC fuel electrodes is relatively small as can be seen in **Figure 1c**.

In this image, a typical impedance spectrum measured on a symmetrical cell at 750 °C (symbols) is plotted together with the obtained fit curve (lines) using the circuit from **Figure 1b**. From the corresponding fit results and the geometry parameters of the electrode, the ionic conductivity and the surface reaction resistance of GDC can be calculated (see Supplemental Experimental Procedure with Figures S1 and S2 for details and more impedance data). At 750 °C, we get an ionic conductivity σ_{ion} = 0.06 S·cm^{-1} and a GDC surface-area-specific resistance R_{react} = 2 Ω·cm^2, which are in excellent agreement with literature values of 0.06 S·cm^{-1} [33] and 4 Ω·cm^2 [34], respectively, thus proving the physical validity of the model. Thanks to the excellent agreement of impedance fitting results to electrode thickness variation (see Supplemental Items (**SI**)) and literature references, we can verify that the GDC phase tortuosity is rather low (~3), compared to values published for Ni-YSZ cermets [35-37]. Due to the very different Ni and GDC particle sizes, most GDC particles are ionically connected, which is most likely the origin of this low tortuosity of the GDC phase. Together with the high GDC surface area, this low tortuosity is jointly responsible for the low anode polarisation resistance and thus the high cell performance.

The respective microstructure of an optimized metal-supported SOFC shown in **Figure 2**, confirms small and homogeneously distributed GDC particles on a coarse Ni network. In addition to high catalytic activity for fuel oxidation, this novel kind of anode microstructure has even further advantages like i.) sufficient mechanical stability and suitably low surface roughness for subsequent electrolyte coating via so-called gas flow sputtering [18], ii.) low risk of Ni coarsening and related degradation phenomena even at operating temperatures up to 800°C and iii.) enhanced redox stability compared to established Ni/YSZ anodes as demonstrated recently [15]. Furthermore, it is expected that this microstructure might be even attractive for operation in electrolysis mode, but related investigations are still pending and part of our future work. For coming to sound conclusions on its suitability, investigation of electrolysis specific degradation phenomena as e.g. reported in literature for solid oxide cells with Ni/YSZ electrode [38,39] will be an important part of this future work.

Stepwise increase of cell performance by improving anode, electrolyte and cathode

Starting from the reference cell (Gen 0) representing the state-of-the-art metal-supported SOFC from Plansee SE with Ni/YSZ anode [17,40,41], the cell was improved stepwise as described in more detail in the **Experimental Procedures**. In Gen 1, the Ni/YSZ anode was replaced by Ni/GDC with optimized microstructure according to our fundamental study described before [19]. The electrochemical performance of the Gen 1 cell confirms the enhanced catalytic activity of the cermet thus proving our approach. Gen 2 features a cell with highly active LSC cathode, therefore increasing catalytic activity also on the air side [20,21] Finally, Gen 3 cell combines for the first time these highly active electrode materials with the thin-film electrolyte and the increased thickness of the active anode layer derived from the basic science section. The electrochemical performance of the Gen 3 cell at operating temperatures between 650 °C and 800 °C is demonstrated in **Figure 3** by current vs. voltage curves (I-V-curves). Due to the outstanding performance of the cell, the maximum current load of the available test rig is exceeded for 0.7 V at each temperature. Therefore, current densities at 0.9 V were chosen for a direct comparison of measured performance values. Additionally, the I-V-curves were extrapolated to a cell voltage of 0.7 V, which is a more common operating point for performance benchmarks. Since the I-V-characteristics show an almost linear behaviour between ca. 1.5 and 2.0 $A \cdot cm^{-2}$, this extrapolation can be done with acceptable accuracy and helps to benchmark the cell performance to published literature. Related extrapolations have already been used before in literature for evaluating SOFC performance [42]. The apparent hysteresis

between the values measured with increasing and decreasing current is due to Joule heating of the cell. To avoid overestimation of the cell performance, the lower values are displayed in the following plots. For details please see the experimental part. At the highest temperature of 800 °C, current densities of 1.77 $A \cdot cm^{-2}$ and 4.47 $A \cdot cm^{-2}$ were measured/extrapolated at 0.9 V and 0.7 V, respectively. This corresponds to power densities of 1.59 $W \cdot cm^{-2}$ and 3.13 $W \cdot cm^{-2}$, which is among the highest ever published values for SOFCs in general and the highest for metal-supported SOFCs in particular.

Figure 4a and **Figure 4b** illustrate the development of cell performance from Gen 0 to Gen 3 for 0.7 V and 0.9 V, respectively. Ultimately, the development of Gen 3 led to an enhancement of the single-cell power density by up to a factor of 10 compared to Gen 0, as also shown in **Figure 4a** and **Figure 4b**. The achieved performance of the highest performing cell type (Gen 3) is compared with results from literature for other metal- as well as anode-supported cells in **Figure 4c** (0.7 V) and **Figure 4d** (0.9 V), revealing a superior performance level of our Gen 3 cells. For a more detailed performance benchmarking with other metal-supported SOFC concepts reported in the literature, the reader is referred to the Supplemental Notes including Table S1.

It is particularly worth emphasizing that the Gen 3 metal-supported cell also outperforms the most advanced anode-supported SOFC (ASC) from Jülich featuring a 1 µm thin electrolyte [42,43], which already served as a major reference value for several SOFC benchmarks. This higher performance despite the larger thickness of the electrolyte confirms the effectiveness of the implemented measures in cell optimization from Gen 0 – Gen 3. Especially the performance boost realized by moving from Gen 2 to Gen 3 emphasizes that microstructure and processing optimization can have an equally important impact on cell performance as introduction of novel electrode materials. Furthermore, by avoiding introduction of completely novel and thus insufficiently characterized materials, the risk of unexpected side effects like unknown, material-specific degradation phenomena is reduced, which is an important aspect for a successful transfer of the technology to industry.

Preliminary testing of long-term stability

Besides the efforts to achieve high-performance cells, preliminary long-term stability tests with humidified fuel gas were conducted using Gen 2 cells. Overall test durations covered up to 1,000 h with more than 400 h of operation under a 50/50 H_2/H_2O mixture as fuel gas. **Figure 5a** shows the long-term behaviour at a current density of 300 $mA \cdot cm^{-2}$. First 230 h of the test were conducted

with dry fuel gas, then the fuel gas was switched to humidified conditions. Another 292 h of operation were achieved with current load under humidified conditions (total humidified period: 432 h). Unfortunately, during this cell test, current and humidification were partly interrupted due to malfunction of the experimental setup, which leads to the somewhat uncommon appearance of the test results in **Figure 5a**. A degradation rate of < 5 mV per 1,000 h was observed indicating that the cell performance was not significantly changed under the given testing conditions. This result was confirmed by I-V measurements in dry and humidified fuel gas before and after continuous operation.

Post-mortem analysis of the Gen 2 cell by SEM after the long-term test revealed a slightly oxidized metal support at the pore walls and at the interface to the GDC diffusion barrier layer. Furthermore, we observed beginning oxidation of Ni grains adjacent to the diffusion barrier layer (**Figure 5b, Figure 5c**) [44]. Energy-dispersive X-ray spectroscopy (EDX) analysis revealed the formation of a Cr_2O_3 scale at positions marked with an arrow. **Figure 5c** hints on increased oxidation of sintering necks, but further investigations are required to conclude on this. In the coarse porous anode layer adjacent to the metal substrate (base layer in **Figure 2**), diffusion of Fe and Cr into the Ni particles was found, which we suggested being the reason of oxide scale formation on the Ni particles (**Figure 5b**). In contrast, Fe and Cr concentration in the active Ni/GDC anode layer was below the detection limit and therefore, we did not observe oxidation of Ni phase in the electrochemically active zone. To clarify when interdiffusion mainly takes place, EDX investigations on as-prepared cells were performed as a reference. These measurements revealed that Fe and Cr diffusion already occurred during sintering of the anode layers mainly due to the higher temperature. The diffusion barrier layer reduced but not completely prevented Fe and Cr diffusion. This observation might be caused by geometrical restrictions at positions where the anode layer penetrates the outer pores of the metal substrate. Caused by the specific coating mechanism of PVD, only the surface of the metal substrate is coated by the diffusion barrier layer.

These preliminary results of operating the cell for 1,000 h at 700°C under humid fuel conditions suggest that the specific cell design of the metal-supported SOFC has the potential for application in real range extender conditions. Since between the Gen 2 and Gen 3 cells only the thickness of both the electrolyte and the anode layer were changed but the materials and processing parameters were kept the same, it is expected that the degradation results of Gen 2 cells can be also regarded as representative for Gen 3. Unfortunately, a related measurement failed due to malfunction of the testing device. In conclusion, we have to admit that the results in the present state are only

preliminary and further systematic long-term tests are required – both in lab conditions as well as in real range extender systems applying a suitable stack design – to draw sound conclusions on the future applicability of this cell concept.

DISCUSSION

Application of metal-supported SOFC technology in range extenders of battery electric vehicles is quite challenging due to limitations in available space. System performance in the range of 20 – 30 kW combined with a volumetric power density (stack level) of 1,000 – 1,200 $W \cdot l^{-1}$ at operation temperatures below 700°C – as aspired by AVL List GmbH on a midterm scale [4] – can only be realized if the current density of the cells exceeds 2 $A \cdot cm^{-2}$ (see Introduction). At the beginning of our target-oriented development of the Plansee SE cell concept in 2016, all published performance values of metal-supported SOFCs were far below this value. For more details, see **Table S1** in the **SI**. Our research hypothesis was to optimize the electrochemically active layers almost independently of each other enabling better understanding of the relationship between processing, microstructure and resulting electrochemical performance for each layer [18-21]. As exemplarily described for the anode in the first part of the Results, in all cases fundamental electrochemical studies on model electrodes were the starting point of development [22,23,29,30,34]. Furthermore, we decided to focus our research on established SOFC materials to avoid unforeseeable degradation phenomena and interface reactions. The improvements achieved by this approach were implemented step by step in the pilot manufacturing at Plansee SE resulting in Gen 1 and Gen 2 cells, which already show current densities near to the target value. In the present work, all efforts were combined for the first time in Gen 3 cells, which are characterized by a Ni/GDC anode, where the thickness was adapted, a 2 µm thin electrolyte and a high performing LSC cathode. As main result of our study, the performance of Gen 3 cells is among the highest ever published values for SOFCs in general and the highest for metal-supported SOFCs in particular (**Figure 4c** and **Figure 4d**). It is expected that system requirements regarding volumetric and gravimetric density can be fulfilled if such current densities can be at least partly transferred to stack level. Our results are – to our opinion – of high interest for other research groups working on SOFC technology since they demonstrate how target-oriented optimization of processing and microstructure of SOFC electrodes can be used to boost electrochemical performance. Especially, the advantage of Ni/GDC anodes and their specific processing resulting in a – compared to full ceramic fuel cells – unconventional microstructure with a coarse and stable Ni network covered by small

interconnected GDC particles might be of interest for other SOFC concepts as well. This microstructure is expected to be quite stable against Ni coarsening and redox cycling. The latter has been proven recently [15]. In the last few years – driven by the automotive industry – significant performance increase was also reported for the cell concepts of Lawrence Berkely National Laboratory (LBNL) [45,46] and Technical University of Denmark (DTU) [47]. For both cell concepts, infiltration technologies were applied to achieve high performing, nanostructured electrodes. It is discussed by the authors that during long-term operation these nanostructures are sensitive to coarsening, which might become the reason for proceeding cell degradation. Another metal-supported SOFC concept is pursued by Ceres Power (UK) focusing on low-cost cell fabrication, rather than maximizing performance [48]. Accordingly, operating conditions and cell requirements differ from other cell concepts. Strategic collaborations in industrial-scale stack manufacturing were established with Weichai Power (China) for range extender development and Robert Bosch GmbH (Germany) for stationary power supply and application in data centers [49]. For more details on running cooperations of Ceres Power, we refer to https://www.cerespower.com. Recently, General Electrics even demonstrated the potential of metal-supported SOFCs for stationary power supply in the several 10 kW range [50]. To achieve stringent cost reduction, they used thermal spray technologies in combination with punched and brazed sheet-metals to overcome traditional stack design constraints. Concerning these multiple industrial activities, it becomes obvious that the relevance of metal-supported technology is not necessarily a matter of mobile applicability, but also considered for stationary systems depending on purpose and boundary conditions. In general, we believe that all results of advanced metal-supported SOFCs are significant for the industrial end-users and decision-makers since they demonstrate the huge potential of the metal-supported SOFC technology for a variety of applications. Furthermore, we believe that some of our results can be easily integrated into other cell concepts like the application of an optimized Ni/GDC anode in the concept of General Electrics.

A novel application of metal-supported SOFCs is the reversible operation in fuel cell and electrolysis mode. Recently, first related results were published by Wang et al. [51]. If operating established full ceramic SOFCs in electrolysis mode, it was reported by several authors that cermet anodes, which are proven for their long-term stability under SOFC conditions, show a specific new degradation phenomenon if operated in electrolysis mode [52-54]. After operation for several 1,000 h in electrolysis mode, agglomeration and depletion of Ni from the electrochemically active zone led to much higher cell degradation than in fuel cell mode. Up to know, the underlying mechanism of

Ni depletion is still unknown. Investigating the electrochemical performance and specific degradation of our optimized Ni/GDC cermet electrode when operated under electrolysis conditions would be of high interest and will be part of our future work.

Up to now, only preliminary electrochemical degradation studies were conducted for evaluation of the long-term stability of the Plansee SE metal-supported SOFC concept. The studies were done on a Gen 2 cell for up to 1,000 h with humidified fuel gas (H_2/H_2O mixture with 50/50 ratio) at 700 °C and a current density of 300 $mA \cdot cm^{-2}$. Under these relatively mild conditions, no obvious cell degradation was observed. This result can be explained as follows. i.) Post-mortem analysis of the cell indicated that growth of Cr_2O_3 scale on the metal support took place at a quite moderate rate. ii.) Even if a GDC diffusion barrier layer is placed between metal support and Ni/YSZ base layer (**Figure 2**), diffusion of Fe and Cr into the Ni phase could not be completely avoided. If exceeding a critical value, Cr in the Ni phase is expected to trigger formation of an electrochemically inactive Cr_2O_3 scale. SEM/EDX analyses of the cell before and after long-term operation [44] reveal that such interdiffusion mainly took place during processing (sintering of the anode layers under H_2 atmosphere at temperatures in the range of 1100°C - 1200°C) and was not aggravated during cell operation. Post-test analysis of the active Ni/GDC anode layer after long-term operation showed very low Cr concentration and no oxidation in this area. iii.) Our specific anode design with coarse porous Ni network and finely dispersed GDC particles on its surface was found to be resistant against further coarsening of microstructure during operation at 700°C. Based on this observation, we expect an advantage regarding long-term stability compared to cell concepts with infiltrated electrodes, but further long-term studies under more realistic range extender conditions are required to prove this assumption.

Whereas suitability for pilot scale manufacturing was confirmed, implementation of the cell in an adapted stack design and testing of these stacks in range extender systems were not demonstrated yet. Therefore, an objective and comprehensive assessment of the suitability of the Plansee SE cell concept for long-term operation under range extender conditions needs to be done in future studies.

In summary, range extender systems for battery electric vehicles powered by SOFCs present a very promising technology for the near-future electrification of the mobility sector, since they enable increased driving range in combination with fast refuelling and reduced size of the required battery. Metal-supported SOFCs, in particular, are predestined to fit the requirements of electromobility such as quick start-up, cyclic operation, and fuel flexibility. However, high performance is a prerequisite for a successful implementation.

Our results demonstrate that suitably combining the efforts of fundamental science and advanced engineering on pilot scale enables major improvement of the electrochemical performance of metal-supported SOFCs. The successful deconvolution of the fuel electrode impedance by using methods of basic electrochemistry provided the understanding for the design of a novel Ni/GDC anode microstructure, which was one of the main keys for the high performance of the metal-supported SOFCs in this work. In accordance with the theoretical calculations, the implementation of finely structured GDC into the fuel electrode and an optimized thickness of the anode layer proved to be a significant measure to enhance cell performance. For the first time, this optimized anode structure was combined with a 2 µm thin-film electrolyte and a highly active LSC cathode, resulting in a performance increase up to a factor of 10 without the need to introduce novel materials. The obtained Gen 3 metal-supported SOFC outperformed even state-of-the-art anode-supported SOFCs, thus setting a new benchmark for SOFC development and demonstrating how an in-depth understanding of fundamental materials properties and their electrochemical interplay provides the basis for a knowledge-based optimization of SOFCs. In addition, preliminary tests confirmed long-term stability of the Gen 2 cells for up to 1,000 h of operation with negligible degradation.

Consequently, metal-supported SOFCs have the potential to play a key role in the implementation of range extender systems in battery electric vehicles. The presented results reveal that microstructure and processing optimization is a strong measure to boost cell performance and encourage other developers of SOFC technology to strengthen efforts on this topic. As the next steps of development, cost reduction of the fabrication, development of a robust stack design and demonstration of long-term stability in a real range extender system are considered most important.

EXPERIMENTAL PROCEDURES

Lead contact

The lead contact of the present work is M.B., Forschungszenntrum Jülich GmbH.

Materials availability

All metal-supported solid oxide fuel cells investigated in this work were produced on pilot scale at Plansee SE. For more details on cell manufacturing, we refer to W.S. and C.S., who are co-authors of this manuscript. Furthermore, we refer to related literature mentioned in the subchapter on manufacturing of metal-supported cells. All processing steps were done on production plants

starting from commercial ceramic and metal powders. For reproducible cell production, Plansee SE applied quality assurance measurements fulfilling industrial standards.

Data and code availability

The authors declare that data supporting the findings of this study are available within the paper and the Supplemental Experimental Procedures including Figure S1 and Figure S2. All other data are available from A.K.O and M.B. upon reasonable request.

Manufacturing of metal-supported fuel cells

All metal-supported SOFCs used in this work were fabricated on a highly porous 300 µm thick ferritic oxide dispersion-strengthened Fe-Cr alloy (Intermediate Temperature Metal ITM from Plansee SE, Austria). The size of the substrates was around 140 x 100 mm ^{2}. For single-cell testing, smaller dimensions of 29 mm Ø or 50 × 50 mm^2 were achieved by laser cutting respective pieces from real full-sized cells. **Figure 6** shows the stepwise change of the Plansee SE cell concept aiming at improving electrochemical performance. For a general description of cell fabrication at Plansee SE, we refer to the literature [17]. In the work of Haydn et al., Gen 0 cells were developed closely mirroring traditional anode-supported cells with Ni/YSZ anode, thin-film 8YSZ electrolyte and $La_{0.58}Sr_{0.4}Fe_{0.2}Co_{0.8}O_{3-\delta}$ (LSCF) cathode. Specific features of the Plansee SE cell concept are a three-layered Ni/YSZ anode with decreasing surface roughness and pore size enabling to coat a gas-tight, 4 µm thick 8YSZ electrolyte via gas flow sputtering. All anode layers were deposited by screen printing starting from mixtures of metallic Ni and 8YSZ powder. It was found that a Ni/YSZ ratio of 80/20 in the top layer was advantageous to achieve high gas tightness of the electrolyte. Sintering of all anode layers was done in reducing H_2 atmosphere at temperatures in the range of 1100 – 1200°C to avoid severe oxidation of the metallic substrate [19]. After sputtering of the electrolyte, the LSCF cathode was screen printed and in situ activated at 800°C during onset of cell operation. To avoid severe interdiffusion at the interfaces, magnetron sputtered GDC barrier layers were deposited between metal support and Ni/YSZ anode and between electrolyte and cathode.

In Gen 1 cells, Ni/GDC was implemented leading to enhanced catalytic activity of the cermet as predicted from fundamental electrochemical studies [19,23]. Lowering the Ni content to 60 wt.% and reduction of sintering temperature to 1100°C was found to be necessary to avoid pronounced Ni coarsening in the presence of GDC. In Gen 2, the in situ activated LSCF cathode was replaced by a highly active $La_{0.58}Sr_{0.4}CoO_{3-\delta}$ (LSC) cathode, significantly increasing catalytic activity also on

the air side. Comprehensive studies were conducted to replace in situ activation by ex situ sintering under protective atmosphere [20] and implementation of LSC/GDC dual-phase cathodes, [21], but best electrochemical performance was still achieved by in situ sintering of LSC. Finally, Gen 3 combines the highly active LSC cathode material with the Ni/GDC anode and thus compiled all efforts to optimize the Plansee SE cell concept in one cell and testing of its electrochemical performance was done for the first time in the present work. Especially, thickness (22 µm) and microstructure of the active Ni/GDC anode were further improved increasing the electrochemically active volume while in parallel enabling deposition of a 2 µm thin-film electrolyte according to the work of Bischof et al. [18]. The increased active layer thickness is a direct consequence of the basic electrochemical investigations (see first part of Results). The region of electrochemical reaction decays from the electrolyte into the porous Ni/GDC anode, and the entire electrochemical reaction takes place within a zone of $3\times\lambda$ ($\lambda=\sqrt{(R_{react}\sigma_{eff})}$; see **SI**). For the optimized Ni/GDC anodes, λ amounts to 5-6 µm (see **Figure S2d**) and thus 15-18 µm active layer thickness are required for fully exploiting their potential. The applied thickness of 22 µm was therefore chosen to safely meet this requirement. Consequently, the Ni/YSZ 65/35 inter- and base layer do not play any role in the electrochemical reaction. Their function is on the one hand to reduce the pore size and roughness from the substrate to the functional layer and on the other hand to collect the electronic current from Ni/GDC.

Electrochemical characterization of Ni/GDC fuel electrodes

For basic characterization of Ni/GDC electrodes, symmetrical electrolyte-supported model cells were fabricated. For details, we refer to the related literature [19]. The symmetrical cells were electrochemically characterized in an atmosphere containing 45 mbar H_2 and 25 mbar H_2O, mimicking 35 % of fuel utilization. The reduced total pressure of 70 mbar was chosen to increase the gas diffusion coefficients, thus suppressing resistive contributions from gas phase diffusion. For impedance measurements, the symmetrical cells were electrically contacted by a highly porous Ni foam in a custom-made sample holder (Huber Scientific, www.sofc.at). Impedance spectroscopy in a frequency range of typically 10 mHz – 1 MHzwas performed at temperatures between ca. 580 °C and 810 °C using a N4L phase sensitive multimeter 1735 with IAI impedance analyser (both: Newtons4th Ltd., www.newtons4th.com).

Quantitative analysis of impedance spectra was done by complex non-linear least squares (CNLS) fitting employing the equivalent circuit in **Figure 1b** (software: Z-View 3.4, Scribner Associates,

Inc., www.scribner.com). Fit results for the Ni/GDC cermet electrode at all experimental temperatures and a comparison of the respective elementary parameters with literature values are shown and discussed in the supporting information.

Electrochemical testing of metal-supported fuel cells

The manufactured metal-supported SOFC full-cells with green (i.e. not sintered) cathode are assembled in the test setup between two thin YSZ frames using a glass sealant developed at Forschungszentrum Jülich [55]. The outer dimensions of the metal support were 50 x 50 mm^2. The size of the active cathode area was 40 x 40 mm^2. During initial heating of the setup, the glass melts and ensures a gas-tight sealing. A dwell time of 10 h at the sealing temperature of 850 °C is set for crystallisation of the sealant and "in situ activation" of the cathode. This term is chosen to differentiate between common sintering processes during cell manufacturing and thermal treatment within the test setup.

Electrochemical characterization is performed using a commercial test rig from EBZ GmbH (Dresden, Germany). Homogeneous gas supply is ensured by the use of a channel design flow field feeding either dry H_2 or a 50/50 H_2/H_2O mixture to the fuel compartment with a flow rate of 1000 sccm H_2. Air is fed to the cathode as an oxidant at 2000 sccm. A Pt mesh is used for the cathode contact and a Ni mesh as current collector at the fuel side. Current-voltage curves are measured from 0-32 A (max 34 A) between 800 °C and 650 °C in steps of 50 K. The maximum fuel utilization amounts to 22 % resulting from the fuel flow rate and the maximum current of the test rig.

IV curves are extrapolated to a theoretical operation point of 0.7 V in order to compare the performance to previous experiments. An extrapolation of the measured data points with a linear slope close to the maximum current load of 2 $A \cdot cm^{-2}$ is used. A possible impact of concentration limitation can be neglected, due to the low fuel utilization of ≤ 22 %. Additionally, benchmarking of measured cell performance is performed at a cell voltage of 0.9 V, to exclude the influence of extrapolation errors. Moreover – as can be seen in **Figure 5** – the high current load leads to an increase of the cell temperature due to Joule heating, which in turn results in an apparent increase of the cell performance visible from the bending of the (otherwise linear) IV curve and a hysteresis-like appearance in the plotted graph between increasing and decreasing current. This is a common issue when testing larger cells but complicates the assessment of extrapolated values.

For a conservative estimate of the presented performance, values for 0.7 V are extrapolated from the data points of decreasing current, whereas the values measured at 0.9 V are derived during

increase of the current. This is as the cell temperature tends to further increase whilst decreasing the current, resulting in a steeper slope and thus in lower current densities extrapolated for 0.7 V. In contrast, the cell temperature is closer to the setpoint during increase of the current load, whereas the progress of the curve while decreasing the current would overestimate the cell performance when relating it to the set temperature.

For estimating the long-term stability of metal-supported SOFCs, electrochemical tests were conducted for up to 1,000 h. In the first seven days, the cell was operated with dry hydrogen. Gen 2 cells were mounted in the test rig and an initial I-V performance check between 800 °C and 650 °C was done at the beginning of the test. Then the cell was continuously operated at 700°C with a current density of 300 $mA \cdot cm^{-2}$ for 100 h. Afterwards, fuel gas composition was changed to a target value of 50 vol.% humidified H_2. I-V curves were measured at 700 °C before and after 100 h operation under dry fuel and at beginning and end of operation with humidified fuel gas, followed by a final performance check using dry fuel.

Acknowledgements

The authors would like to thank T. Brambach and C. Tropartz for conducting the electrochemical tests, and Dr D. Sebold for SEM analysis. Furthermore, the authors gratefully acknowledge funding of the Christian Doppler Laboratory for Interfaces in Metal-supported Electrochemical Energy Converters by the Austrian Federal Ministry for Digital and Economic Affairs (BMDW) and the National Foundation for Research, Technology and Development.

Author Contributions

Conceptualization: M.B., W.S., J.R., and A.K.O.; Methodology: M.B. and A.K.O.; Investigation: D.U., C.B., F.T., and A.N.; Resources: W.S., N.H.M., L.G.J.D.H., A.K.O., and M.B.; Writing – Original Draft: D.U., A.K.O., A.N. and M.B.; Writing – Review & Editing: R.N., W.S., N.H.M., and O.G.; Visualization: D.U., M.B., A.N., and A.K.O.; Supervision: M.B., A.K.O., J.R., and W.S.; Project Administration: M.B. and A.K.O; Funding Acquisition: M.B., A.K.O., J.R. and W.S.

Conflicts of Interest

Plansee SE and AVL List GmbH do have an interest in successful commercialization of SOFC-powered range extender systems. However, since this technology is not yet available on the market, there will be no direct benefits for the companies from publication of this study. Rather, we intend to inspire the scientific community to further pushing this technology forward and developing their SOFC systems accordingly.

Literature

1. McCollum DL, Wilson C, Bevione M, Carrara S, Edelenbosch OY, Emmerling J, Guivarch C, Karkatsoulis P, Keppo I, Krey V, et al. (2018) Interaction of consumer preferences and climate policies in the global transition to low-carbon vehicles. Nature Energy 3(8), 664-673.
2. Rechberger J, Reissig M, Lawlor V, (2018) SOFC EV range extender systems for biofuels (Springer Fachmedien Wiesbaden).
3. Cano ZP, Banham D, Ye S, Hintennach A, Lu J, Fowler M, Chen Z. (2018) Batteries and fuel cells for emerging electric vehicle markets. Nature Energy 3(4), 279-289.
4. Lawlor V, Reissig M, Makinson J, Rechberger J. (2017) SOFC System for Battery Electric Vehicle Range Extension: Results of the First Half of the Mestrex Project. ECS Transactions 78(1), 191-195.
5. (2016) MeStREx project uses ethanol fueled SOFCs in EV range-extenders. Fuel Cells Bulletin 2016(11), 2-3.
6. Brett DJL, Atkinson A, Brandon NP, Skinner SJ. (2008) Intermediate temperature solid oxide fuel cells. Chemical Society Reviews 37(8), 1568-1578.
7. Eguchi K, Kojo H, Takeguchi T, Kikuchi R, Sasaki K. (2002) Fuel flexibility in power generation by solid oxide fuel cells. Solid State Ionics 152–153, 411-416.
8. Reissig M, Mathé J, Planitzer S, Vötter R, Rechberger J. (2015) Standalone Portable SOFC Power Generator for Autonomous Operation. ECS Transactions 68(1), 143-150.
9. Tucker MC. (2010) Progress in metal-supported solid oxide fuel cells: A review. Journal of Power Sources 195(15), 4570-4582.
10. Glenk G, Reichelstein S. (2019) Economics of converting renewable power to hydrogen. Nature Energy 4(3), 216-222.
11. DOE. (2012) Fuel Cell Technologies Office Multi-Year Research, Development, and Demonstration Plan. (U.S. Department of Energy's).
12. Botti JJ. (2003) The Revolution Through Evolution: Delphi Solid Oxide Fuel Cell for APU and Hydrogen Reformation. ECS Proceedings Volumes 2003-07(1), 16-30.
13. Botti JJ, Grieve MJ, MacBain JA. (2005) Electric Vehicle Range Extension Using an SOFC APU. SAE 2005 World Congress & Exhibition (SAE International).
14. Krishnan VV. (2017) Recent developments in metal-supported solid oxide fuel cells. Wiley Interdisciplinary Reviews: Energy and Environment.
15. Thaler F, Udomsilp D, Schafbauer W, Bischof C, Fukuyama Y, Miura Y, Kawabuchi M, Taniguchi S, Takemiya S, Nenning A, et al. (2019) Redox stability of metal-supported fuel cells with nickel/gadolinium-doped ceria anode. Journal of Power Sources 434, 226751.
16. Boldrin P, Brandon NP. (2019) Progress and outlook for solid oxide fuel cells for transportation applications. Nature Catalysis 2(7), 571-577.
17. Haydn M, Ortner K, Franco T, Uhlenbruck S, Menzler NH, Stöver D, Bräuer G, Venskutonis A, Sigl LS, Buchkremer H-P, et al. (2014) Multi-layer thin-film electrolytes for metal supported solid oxide fuel cells. Journal of Power Sources 256, 52-60.
18. Bischof C, Nenning A, Malleier A, Martetschläger L, Gladbach A, Schafbauer W, Opitz AK, Bram M. (2019) Microstructure optimization of nickel/gadolinium-doped ceria anodes as key to significantly increasing power density of metal-supported solid oxide fuel cells. International Journal of Hydrogen Energy 44(59), 31475-31487.
19. Rojek-Wöckner VA, Opitz AK, Brandner M, Mathé J, Bram M. (2016) A novel Ni/ceria-based anode for metal-supported solid oxide fuel cells. Journal of Power Sources 328, 65-74.
20. Udomsilp D, Roehrens D, Menzler NH, Bischof C, de Haart LGJ, Opitz AK, Guillon O, Bram M. (2017) High-Performance Metal-Supported Solid Oxide Fuel Cells by Advanced Cathode Processing. Journal of The Electrochemical Society 164(13), F1375-F1384.

21. Udomsilp D, Thaler F, Menzler NH, Bischof C, de Haart LGJ, Opitz AK, Guillon O, Bram M. (2019) Dual-Phase Cathodes for Metal-Supported Solid Oxide Fuel Cells: Processing, Performance, Durability. Journal of The Electrochemical Society 166(8), F506-F510.
22. Gerstl M, Nenning A, Iskandar R, Rojek-Wöckner V, Bram M, Hutter H, Opitz A. (2016) The Sulphur Poisoning Behaviour of Gadolinia Doped Ceria Model Systems in Reducing Atmospheres. Materials 9(8), 649.
23. Opitz AK, Gerstl M, Bram M. (2019) Model System Supported Impedance Simulation of Composite Electrodes. Fuel Cells 19(4), 417-428.
24. Mogensen M, Sammes NM, Tompsett GA. (2000) Physical, chemical and electrochemical properties of pure and doped ceria. Solid State Ionics 129(1), 63-94.
25. Tuller HL, Nowick AS. (1977) Small polaron electron transport in reduced CeO2 single crystals. Journal of Physics and Chemistry of Solids 38(8), 859-867.
26. Chueh WC, Hao Y, Jung W, Haile SM. (2011) High electrochemical activity of the oxide phase in model ceria–Pt and ceria–Ni composite anodes. Nature Materials 11, 155.
27. Adler SB, Lane JA, Steele BCH. (1996) Electrode Kinetics of Porous Mixed-Conducting Oxygen Electrodes. Journal of The Electrochemical Society 143(11), 3554-3564.
28. Nielsen J, Jacobsen T, Wandel M. (2011) Impedance of porous IT-SOFC LSCF:CGO composite cathodes. Electrochimica Acta 56(23), 7963-7974.
29. Nenning A, Gerstl M, Bram M, Opitz AK. (2019) Mechanistic Insight into Porous Electrode Impedance: An Example of Ni+YSZ Cermet Anodes. ECS Transactions 91(1), 479-490.
30. Nenning A, Bischof C, Fleig J, Bram M, Opitz AK. (2020) The Relation of Microstructure, Materials Properties and Impedance of SOFC Electrodes: A Case Study of Ni/GDC Anodes. Energies 13(4), 987.
31. Chueh WC, Haile SM. (2009) Electrochemical studies of capacitance in cerium oxide thin films and its relationship to anionic and electronic defect densities. Physical Chemistry Chemical Physics 11(37), 8144-8148.
32. Jamnik J, Maier J. (2001) Generalised equivalent circuits for mass and charge transport: chemical capacitance and its implications. Physical Chemistry Chemical Physics 3(9), 1668-1678.
33. Wang S, Kobayashi T, Dokiya M, Hashimoto T. (2000) Electrical and Ionic Conductivity of Gd-Doped Ceria. Journal of The Electrochemical Society 147(10), 3606-3609.
34. Gerstl M, Hutterer A, Fleig J, Bram M, Opitz AK. (2016) Model composite microelectrodes as a pathfinder for fully oxidic SOFC anodes. Solid State Ionics 298, 1-8.
35. Iwai H, Shikazono N, Matsui T, Teshima H, Kishimoto M, Kishida R, Hayashi D, Matsuzaki K, Kanno D, Saito M, et al. (2010) Quantification of SOFC anode microstructure based on dual beam FIB-SEM technique. Journal of Power Sources 195(4), 955-961.
36. Izzo JR, Joshi AS, Grew KN, Chiu WKS, Tkachuk A, Wang SH, Yun W. (2008) Nondestructive Reconstruction and Analysis of SOFC Anodes Using X-ray Computed Tomography at Sub-50 nm Resolution. Journal of The Electrochemical Society 155(5), B504-B508.
37. Kanno D, Shikazono N, Takagi N, Matsuzaki K, Kasagi N. (2011) Evaluation of SOFC anode polarization simulation using three-dimensional microstructures reconstructed by FIB tomography. Electrochimica Acta 56(11), 4015-4021.
38. Mogensen MB, Hauch A, Sun X, Chen M, Tao Y, Ebbesen SD, Hansen KV, Hendriksen PV. (2017) Relation Between Ni Particle Shape Change and Ni Migration in Ni–YSZ Electrodes – a Hypothesis. Fuel Cells 17(4), 434-441.
39. Tao Y, Ebbesen SD, Mogensen MB. (2016) Degradation of solid oxide cells during co-electrolysis of steam and carbon dioxide at high current densities. Journal of Power Sources 328, 452-462.
40. Franco T, Haydn M, Mücke R, Weber A, Rüttinger M, Büchler O, Uhlenbruck S, Menzler NH, Venskutonis A, Sigl LS. (2011) Development of Metal-Supported Solid Oxide Fuel Cells. ECS Transactions 35(1), 343-349.

41. Franco T, Haydn M, Weber A, Schafbauer W, Blum L, Packbier U, Roehrens D, Menzler NH, Rechberger J, Venskutonis A, et al. (2013) The Status of Metal-Supported SOFC Development and Industrialization at Plansee. ECS Transactions 57(1), 471-480.
42. Han F, Mücke R, Van Gestel T, Leonide A, Menzler NH, Buchkremer HP, Stöver D. (2012) Novel high-performance solid oxide fuel cells with bulk ionic conductance dominated thin-film electrolytes. Journal of Power Sources 218(0), 157-162.
43. Blum L, de Haart LGJ, Malzbender J, Menzler NH, Remmel J, Steinberger-Wilckens R. (2013) Recent results in Jülich solid oxide fuel cell technology development. Journal of Power Sources 241, 477-485.
44. Thaler F, Nenning A, Bischof C, Udomsilp D, de Haart LGJ, Opitz AK, Bram M. (2019) Optimized Cell Processing as the Key of High Electrochemical Performance of Metal-Supported Solid Oxide Fuel Cells. ECS Transactions 91(1), 887-900.
45. Dogdibegovic E, Wang R, Lau GY, Tucker MC. (2019) High performance metal-supported solid oxide fuel cells with infiltrated electrodes. Journal of Power Sources 410-411, 91-98.
46. Tucker MC. (2017) Development of High Power Density Metal-Supported Solid Oxide Fuel Cells. Energy Technology 5(12), 2175-2181.
47. Nielsen J, Persson ÅH, Muhl TT, Brodersen K. (2018) Towards High Power Density Metal Supported Solid Oxide Fuel Cell for Mobile Applications. Journal of The Electrochemical Society 165(2), F90-F96.
48. Leah RT, Bone A, Hammer E, Selcuk A, Rahman M, Clare A, Rees L, Lawrence N, Ballard A, Domanski T, et al. (2017) Development of High Efficiency Steel Cell Technology for Multiple Applications. ECS Transactions 78(1), 2005-2014.
49. (2018) Ceres Power, Bosch in strategic collaboration, prepare for production. Fuel Cells Bulletin 2018(9), 11.
50. Hickey D, Alinger M, Shapiro A, Brown K, Striker T, Wang H, Gaunt S, Kinsey D, Hussaini I. (2017) Stack Development at GE-Fuel Cells. ECS Transactions 78(1), 107-116.
51. Wang R, Dogdibegovic E, Lau GY, Tucker MC. (2019) Metal-Supported Solid Oxide Electrolysis Cell with Significantly Enhanced Catalysis. Energy Technology 7(5), 1801154.
52. Hoerlein MP, Riegraf M, Costa R, Schiller G, Friedrich KA. (2018) A parameter study of solid oxide electrolysis cell degradation: Microstructural changes of the fuel electrode. Electrochimica Acta 276, 162-175.
53. Fang Q, Frey CE, Menzler NH, Blum L. (2018) Electrochemical Performance and Preliminary Post-Mortem Analysis of a Solid Oxide Cell Stack with 20,000 h of Operation. Journal of The Electrochemical Society 165(2), F38-F45.
54. Frey CE, Fang Q, Sebold D, Blum L, Menzler NH. (2018) A Detailed Post Mortem Analysis of Solid Oxide Electrolyzer Cells after Long-Term Stack Operation. Journal of The Electrochemical Society 165(5), F357-F364.
55. Gross SM, Koppitz T, Remmel J, Bouche J-B, Reisgen U. (2006) Joining properties of a composite glass-ceramic sealant. Fuel Cells Bulletin 2006(9), 12-15.
56. Klemensø T, Nielsen J, Blennow P, Persson ÅH, Stegk T, Christensen BH, Sønderby S. (2011) High performance metal-supported solid oxide fuel cells with Gd-doped ceria barrier layers. Journal of Power Sources 196(22), 9459-9466.

Figures

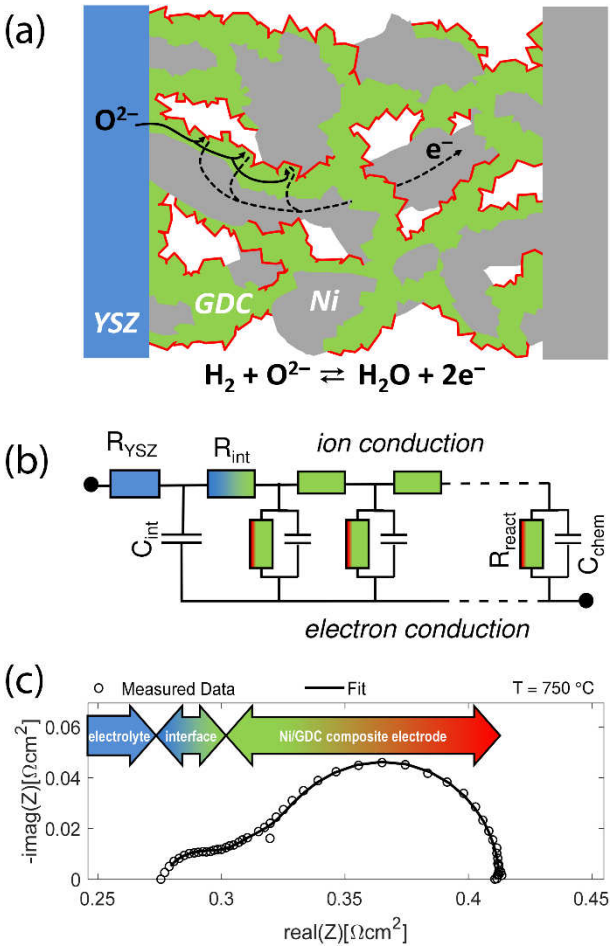

Figure 1. Predicting optimum microstructure of Ni/GDC cermets by a fundamental electrochemical approach

Electrochemical performance of the fuel electrode. **(a)** Sketch of the current pathways in the Ni/GDC cermet for oxide ions (solid arrows) and electrons (dashed arrows). The electrochemical fuel oxidation reaction proceeds on the free GDC surface, which is highlighted by the red colour. **(b)** Equivalent circuit representing the electrochemical current pathways and the physical elementary parameters of the involved materials. For a percolating Ni phase, the resistances of the electronic rail are very small (σ_{eon} of Ni is ca. 10^5 S cm^{-1}); for fitting purposes, this rail was thus short-circuited. **(c)** Typical impedance spectrum (Nyquist plot) measured on a symmetrical model cell with 6 µm thick Ni/GDC cermet anode (circles) together with fit curve (line) employing the circuit in **(b)**. To demonstrate the reproducibility of the anode impedance and to show the effect of different functional layer thickness, additional impedance results are shown in the SI, Figures S1 and S2.

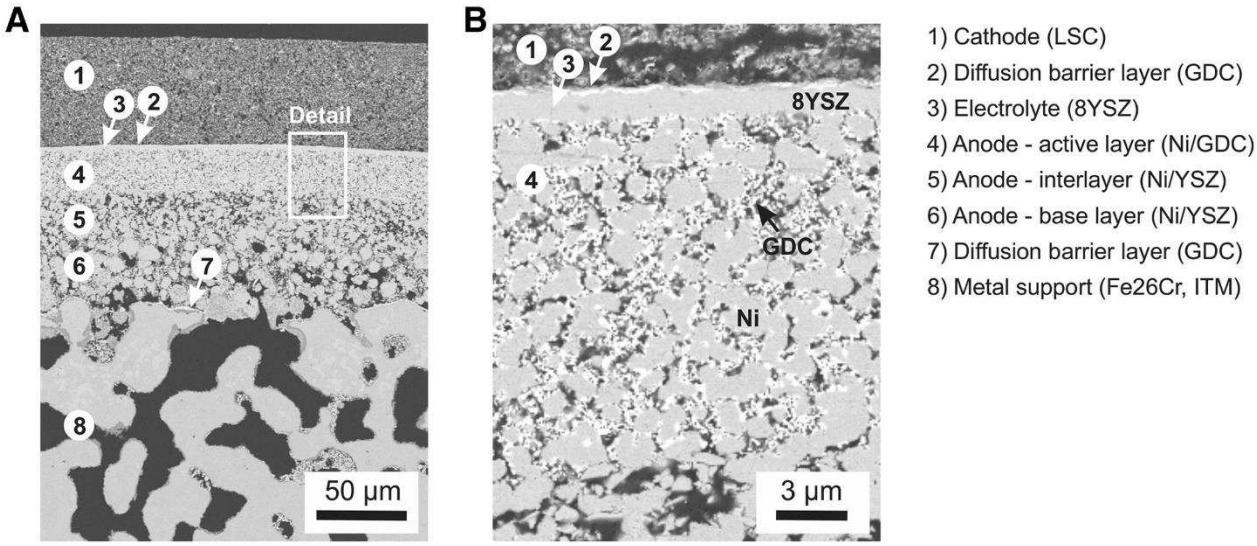

Figure 2. Implementation of Ni/GDC cermet electrode with optimized microstructure in Gen 3 cells

Microstructure of a Gen 3 metal-supported SOFC **(a)** cross-section showing all layers of the cell, **(b)** optimized Ni/GDC anode design with coarse Ni network and finely dispersed, electrochemically active GDC phase (large grey particles: Ni – small white particles: GDC).

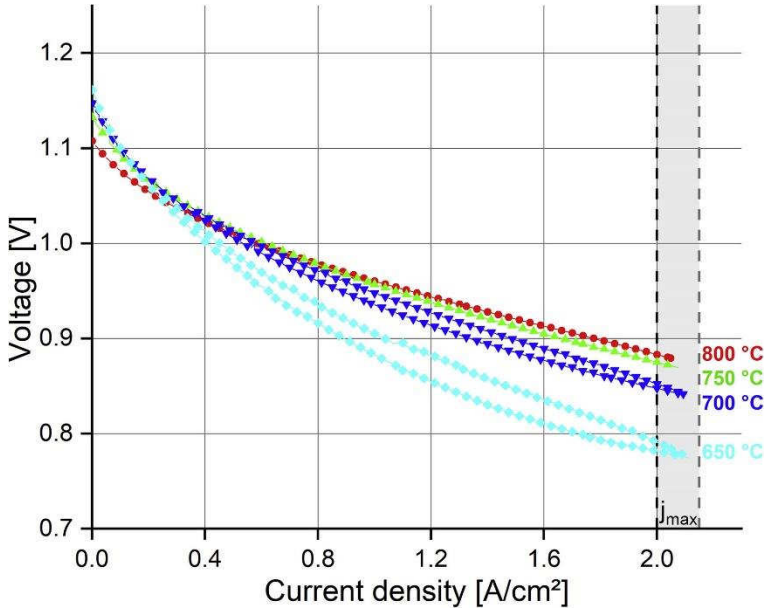

Figure 3. Electrochemical performance of Gen 3 cells

I-V-characteristics of the Gen 3 metal-supported SOFC at operating temperatures between 650 °C and 800 °C. 50 × 50 mm^2 cell with 16 cm^2 active cathode area. Gas supply – 1000 sccm H_2, 2000 sccm air.

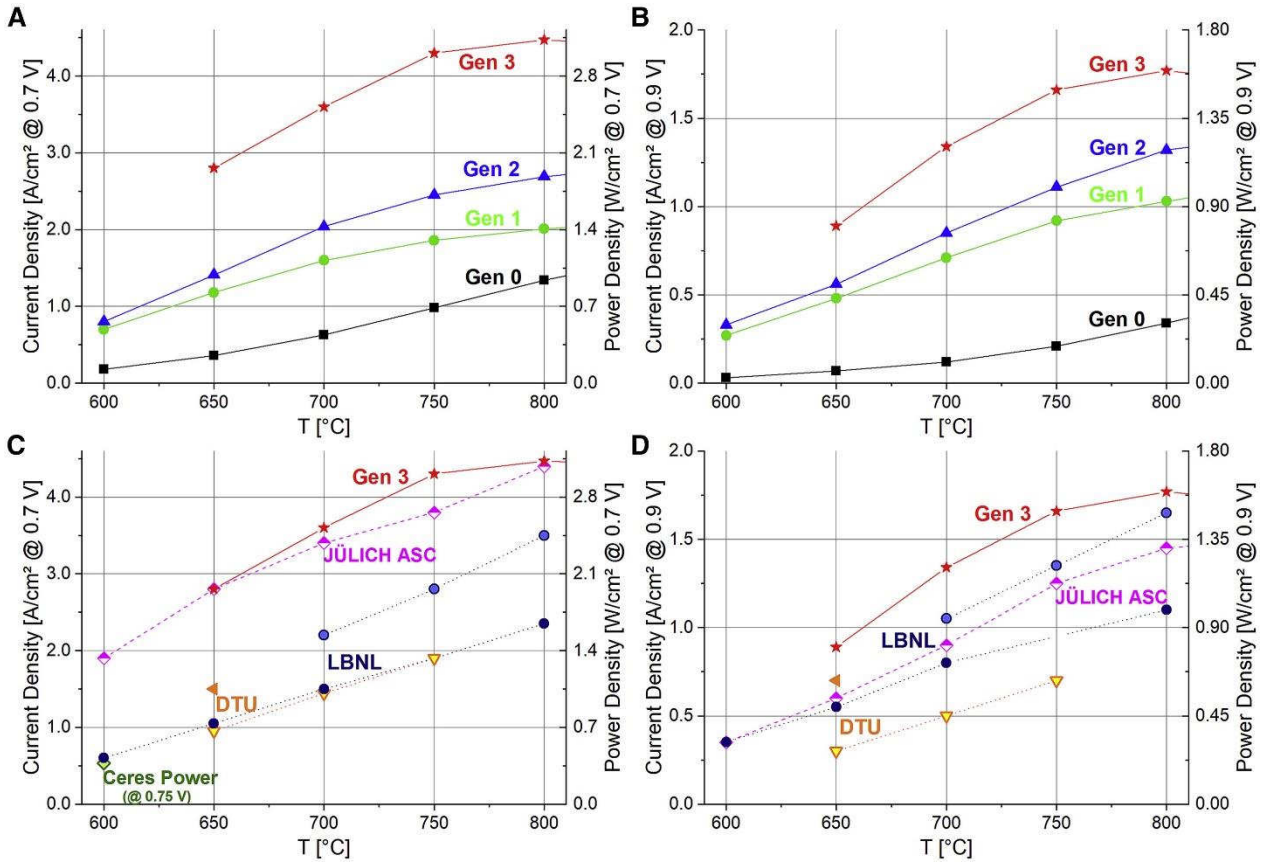

Figure 4. Evolution of electrochemical performance from Gen 0 to Gen 3 cells and benchmark to other cell concepts

Increase of current and power density by systematic processing and microstructure optimization of the metal-supported SOFC in 3 cell generations at cell voltages of **(a)** 0.7 V and **(b)** 0.9 V. Performance benchmark by comparison of Gen 3 with literature data of the JÜLICH ASC [42,43] and metal-supported SOFCs from LBNL [45,46], DTU [47,56], and Ceres Power [48] at cell voltages of c) 0.7 V and d) 0.9 V. For a more detailed benchmark of published MSC results see Table S1.

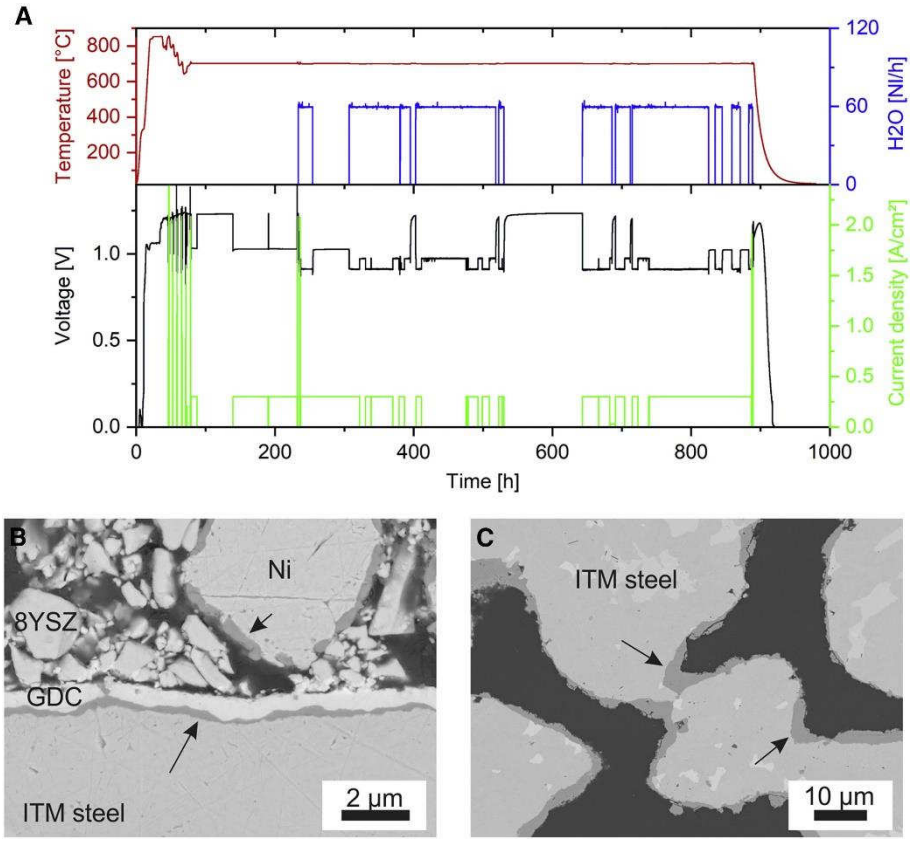

Figure 5. Preliminary long-term test of Gen 2 cells with humidified fuel gas

(a) Cell voltage of a Gen 2 cell (Ni/GDC anode functional layer, LSC cathode) during a two-step degradation test at 700 °C and constant current load of 300 mA cm ² over 900 h. First period: dry H_2 fuel. Second period: 50 % humidified H_2. Post-mortem analysis after cell test showed **(b)** formation of Cr_2O_3 scales at the interface to the diffusion barrier layer and adjacent Ni grains and **(c)** increased formation of Cr_2O_3 scales at sintering necks. Cr_2O_3 scales were analyzed by EDX and are marked by arrows. Adapted from [44].

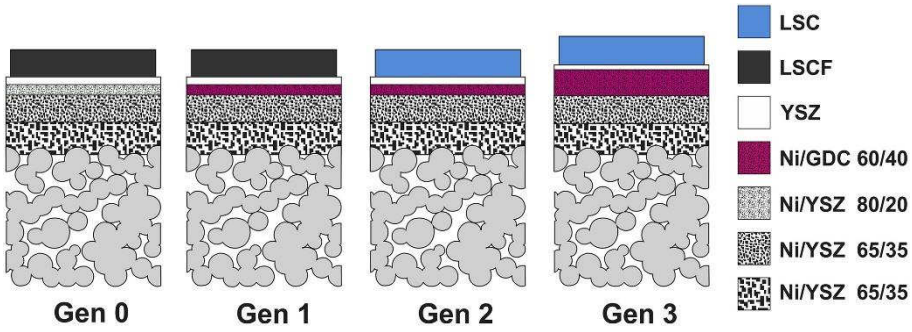

Figure 6. Evolution of the metal-supported solid oxide fuel cell concept being in the focus of this work

Schematic of the implemented measures for enhancing performance of metal-supported SOFCs (Plansee SE concept) in three cell generations. Ni/ceramic ratio given in wt.-%.